Nanoscale

RSC Publishing

COMMUNICATION

View Article Online
View Journal

Wafer scale fabrication of porous three-dimensional plasmonic metamaterials for the visible region: chiral and beyond†

Cite this: DOI: 10.1039/c3nr02666c

Received 22nd May 2013
Accepted 15th June 2013

DOI: 10.1039/c3nr02666c

www.rsc.org/nanoscale

Johnson Haobijam Singh,*[a] Greshma Nair,[b] Arijit Ghosh[c] and Ambarish Ghosh*[abc]

We report on a wafer scale fabrication method of a three-dimensional plasmonic metamaterial with strong chiroptical response in the visible region of the electromagnetic spectrum. The system was comprised of metallic nanoparticles arranged in a helical fashion, with high degree of flexibility over the choice of the underlying material, as well as their geometrical parameters. This resulted in exquisite control over the chiroptical properties, most importantly the spectral signature of the circular dichroism. In spite of the large variability in the arrangement, as well as the size and shape of the constituent nanoparticles, the average chiro-optical response of the material remained uniform across the wafer, thus confirming the suitability of this system as a large area chiral metamaterial. By simply heating the substrate for a few minutes, the geometrical properties of the nanoparticles could be altered, thus providing an additional handle towards tailoring the spectral response of this novel material.

Naturally occurring optically active media, such as a collection of chiral molecules, typically exhibit weak differential response to circularly polarized light.[1] This is in contrast to certain artificial chiral materials, especially those relying on strong light–matter interactions in plasmonic nanostructures, whose optical activity can be engineered to be several orders of magnitude stronger than any naturally occurring substance. Possible applications for such metamaterials[2,3] with strong chiro-optical response include media with negative refractive index,[4,5] photonic devices such as broadband circular polarizers,[6] sensors[7] for chiral molecules and offer a rich platform to enhance and study the interaction of polarized light with chiral bio-complexes. The working principles[8] behind most recent chiral metamaterials rely on strong light–matter interactions in a metallic nanostructure of chiral shape, or a chiral assembly of metallic nanostructures, where most commonly the handedness is introduced through a helical shape, a text book example of a chiral geometry. Few of the current methods used to fabricate such systems allow very high flexibility in obtaining a wide range of geometrical parameters, which have been used to develop optical metamaterials with large and well designed chiroptical properties. Unfortunately, all these methods rely on sequential lithographic steps,[9,10] and are therefore not suitable for the development of wafer scale devices of technological importance. This is in contrast to certain highly scalable[11] fabrication schemes, such as those based on decorating[12–14] chiral (helical) nanostructures with metallic nanoparticles, which though scalable, allow limited freedom in choosing the geometrical properties of the chiral geometry. In this paper, we demonstrate a new technique of wafer scale fabrication of chiral and other three-dimensional plasmonic metamaterials, with unprecedented freedom in designing the geometrical and spectral characteristics of the medium, and obtained an optical response whose strength was on a par with the highest that has been achieved to date in the visible range of the electromagnetic spectrum. It is important to note that there have been other chiro-plasmonic materials[6,10,15] with even higher chiro-optical response than the material described here, but none in the visible region of the spectrum. This is partially related to the methods used to fabricate these systems, such as electron-beam or two-photon lithography, which limited the minimum available sizes of the constituent plasmonic elements, thereby resulting in plasmonic resonance in the near or mid-IR region. This limitation has been overcome in the present system.

The wafer scale approach presented here relied on the placement of plasmonic nanoparticles (NPs) in three dimensions, with exquisite control over the geometrical parameters of the NP arrangement. The plasmonic interactions between the NPs could thus be designed with great precision, resulting in a

[a]*Department of Physics, Indian Institute of Science, Bangalore, 560012, India. E-mail: johnsonthonga196@gmail.com*

[b]*Centre for Nano Science and Engineering, Indian Institute of Science, Bangalore, 560012, India. E-mail: ambarish@ece.iisc.ernet.in*

[c]*Department of Electrical Communications Engineering, Indian Institute of Science, Bangalore, 560012, India*

† Electronic supplementary information (ESI) available: Experimental procedure (fabrication and characterization); effect of linear dichroism; chiroptical response for isotropic collection of helices; details of the computational model; thickness dependent red shift. See DOI: 10.1039/c3nr02666c

well engineered optical response of the metamaterial. As proof of principle, we have demonstrated strong chiro-optical properties arising out of a helical arrangement of Ag and Au NPs, although the method could easily be extended to various other three-dimensional variants as well. Our technique was based on a subtle innovation over the well known shadow evaporation method, also known as Glancing Angle Deposition[16,17] (GLAD), which has hitherto been used to fabricate nanostructured thin films (including chiral[18]) based on various dielectrics. The integration of metals to this technique is not trivial, as surface diffusion of the highly mobile metal atoms destroys the self-shadowing mechanism that lies at the heart of this technique. Accordingly, previous attempts to integrate plasmonics onto structures grown by GLAD have been mostly limited to metallic nanorods,[19] metal films grown on dielectric rods[20] and very recently, alternate layers[21] of metals and dielectric nano-discs, none of which could give rise to a well defined chiral arrangement of metal NPs of sub-10 nm dimensions. The small size of the NPs is of paramount importance in engineering the chiro-optical response in the visible part of the spectrum, assuming that we are limited to common plasmonic materials, such as gold and silver.

The first step of the fabrication method was to use the conventional method of GLAD to make a template of the chosen geometry with any suitable dielectric, such as SiO_2, MgF_2 *etc.* A rotating substrate was kept at an extreme tilt angle of 84° to the incoming source of vapour, in order to grow a helically nanostructured dielectric film. In the second and the most crucial fabrication step, the tilt of the substrate was reduced to around 5°, and subsequently a small quantity of metal was evaporated (see Fig. 1A). Under these conditions, the surface of the helices was effectively at an extreme angle to the incoming metal vapour, which for low thickness of the evaporated material, formed isolated metallic islands on the surface of the helix through self-shadowing. This being a line of sight technique, the metallic NPs were placed along a chiral geometry, defined by the geometrical parameters of the dielectric helix. The size, shape, position and number of NPs depended on the thickness of the metallic film, as well as the helix geometry, and as discussed later, could be further controlled by heating the substrate. SEM images of the helical film, with and without the NPs, are shown in Fig. 1B. The metallic islands arranged on the helical nanostructures could be seen as white dots, whose sizes and shapes depend strongly on the thickness of the metallic film deposited. Strong plasmonic effects gave rise to uniform bright colours throughout the substrate which varied from almost colourless to dark yellow (see Fig. 1C) as the amount of the evaporated metal (Ag here) was increased. While there was variability in number, size, spacing and separation between the Ag NPs assembled on individual helices, the density of the helices within a single wavelength of light was very large, almost 350 μm^{-2}, thus resulting in high uniformity in the measured optical properties across the surface of the samples. All the films exhibited large circular dichroism (CD), where CD is defined as the difference in extinction for left (A_L) and right (A_R) circularly polarized (cp) light, given by $CD = A_L - A_R = \log(I_R/I_L) \approx 2\,(I_L - I_R)/(I_L + I_R)$ (valid for small $I_L - I_R$) and is obtained as the ratio of two measurable quantities, the difference between intensities of the transmitted light for the two cp components ($I_L - I_R$) to the average transmitted intensity ($= (I_L + I_R)/2$). We ensured that the linear dichroism (LD) from the samples had negligible contribution to the measured CD values (details in the ESI†). The mechanism of optical extinction in this system was dominated by absorption (with minimal scattering losses), as expected for a system of Ag (or Au) NPs of sub-10 nm dimensions. We measured the circular differential scattering from the helical template made of silica,[22] and found the effect to be negligible compared to what was observed when the metal NPs were added. A better estimate of the strength of the chiral interaction is the anisotropy factor, defined as $g = \Delta A/A$, where ΔA and A refer to the circular differential and average extinctions respectively. For all the films shown here, the value of g was around 20%, implying a stronger chiro-optical response in the visible region than most plasmonic systems developed so far.

The spectral characteristics of the CD spectrum showed a strong dependence on the thickness of the metal film (see Fig. 1D), with large spectral widths (FWHM ~ 150 nm) across the visible region of the electromagnetic spectrum, where the thickness dependent red shift was related mainly to the larger sizes, close spacing and ellipticities of the metallic islands at higher film thicknesses (see the ESI†). The chiro-optical response, as expected, reversed its sign when the handedness of the helix was reversed, also shown in Fig. 1D. These measurements were done for a film with an incident beam along the axes of the helices, and the resultant chiroptical signal mostly arose out of plasmonic interactions between Ag NPs belonging to the same helix. This is because the smallest distance between particles on two neighbouring helices (>60 nm) is far more than

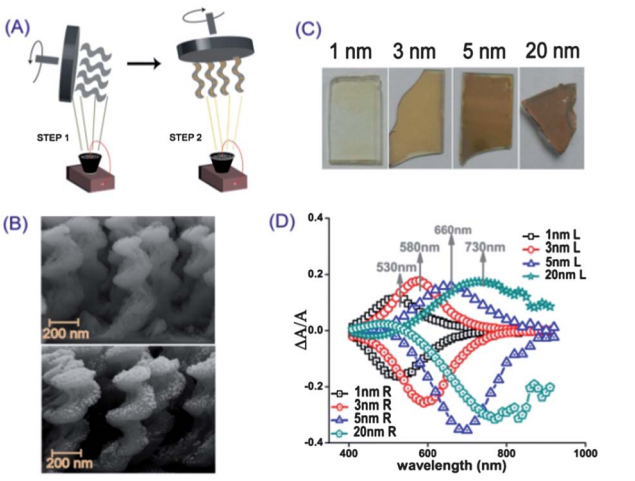

Fig. 1 (A) Schematic of the fabrication method, where conventional GLAD is used to fabricate the dielectric 3D template in the first step, followed by an evaporation of metallic islands in the second step. (B) SEM images of the nanostructured surfaces without (top) and with (bottom) the Ag metallic islands. (C) Digital photographs of the samples under white light illumination. The thickness of the Ag metal layer is shown. (D) Chiral anisotropy factor $\Delta A/A$ *vs.* wavelength for various thicknesses of the Ag metal layer for both Left (L) and Right (R) handed samples. Gradual shifts of the peak wavelengths have been marked.

typical nanoparticle separations within the same helix (~2 to 8 nm), implying that plasmonic coupling between two neighbouring helices may be neglected. We have also measured the chiroptical response of an isotropic collection (see the ESI†) of the helices, obtained by sonicating the structures in water. The isotropic collection showed a dip-peak[13,14] shape that had been experimentally observed before in other isotropic arrangements of chiro-plasmonic structures. For the light beam incident along an arbitrary direction with respect to the axis of the helix, dipolar modes along and perpendicular to the axis were excited, resulting in CD signals of opposite signs. The energies of these modes were slightly different, which resulted in the observed dip-peak shape of the CD spectrum in the isotropic collection, but could not be observed in a film where the helices were all oriented along the direction of the incident light beam. This also resulted in the strength of the film CD to be almost an order of magnitude higher compared to the isotropic collection of helices, although the number of helices interacting with the light beam was approximately the same in both cases.

An obvious advantage of the technique described here is the ease and scalability of the fabrication method allowing the development of wafer scale 3D metamaterials with strong and spectrally wide chiro-optical response. However, engineering the plasmonic coupling between the metallic islands arranged along the helical geometry defining this material is not easy due to the large variability in the sizes and shapes of these metallic islands, which would limit how well the optical response of the material could be designed. Our solution to this problem was to simply heat the substrates, which resulted in a dramatically increased sphericity of the metallic islands. SEM images of the metallic islands before and after the heating step are shown in Fig. 2A, where the reduction of NP ellipticities upon heating[23,24] could be easily observed. The corresponding optical properties of the material had a large visual change (see photographs in Fig. 2B) for both Au and Ag coated helical films, while the chiro-optical spectrum showed a distinct shift to the blue. The observation of the thickness dependent red shift (see Fig. 1D), as well as the blue shift upon heating (see Fig. 2C), both point towards the relation of the chiro-optical spectrum to the sphericity of the constituent NPs, and is qualitatively similar to the previously reported dependence of the CD spectrum on the aspect ratio of gold nanorods organized in chiral supramolecular fibers.[13]

The random sizes, shapes and spacings of the unheated metallic islands (shown in Fig. 2A) were difficult to model using numerical methods, and therefore not suitable from the perspective of engineering a chiro-optical material with well designed properties. In this regard, the heated substrates, although showed a slightly lower chiral anisotropy factor, formed an ideal experimental system that could be modelled with theoretical tools. While it is possible to model a system of NPs arranged in a helical geometry using standard computational tools, such as those based on FEM, FDTD *etc.*, investigating the effects of variability of different geometrical parameters requires tremendous computational resources. A simpler and possibly more insightful option that allows a thorough investigation of the impact of geometrical variation is to use a semi-analytical approach, for example a model based on coupled dipole approximation[25–27] (CDA). This scheme closely resembles the physical mechanism that gave rise to the chiro-optical response observed in the experimental system, originating from the dynamic Coulomb interaction[25,28] between NPs arranged in a chiral geometry. In essence, each NP could be considered to have a net dipole moment induced by the electric field of the incident electromagnetic wave and the electric field due to all other dipoles. The strong near field coupling between the dipoles arranged in a chiral geometry could thereby result in the strong chiro-optical response observed here. It should be noted that additional effects could arise due to the far field[29,30] electromagnetic coupling of the metal NPs and the chiral dielectric template, an effect that cannot be incorporated within the limits of the present numerical scheme. Also note that applicability[31] of the coupled dipole approximation is limited to arrangements of NPs whose centre-to-centre distances (r) are more than three times their sizes (a), while the r/a ratios of the geometries discussed here were always less than three. Furthermore, the system presented here was comprised of two types of dielectric, *e.g.* SiO_2 for the helical structure, and air (or water) in the region between the helices, which is difficult to implement with this method. In spite of these differences between the real system and what could be modelled with CDA, we could understand certain important aspects of the chiro-optical spectrum using CDA based calculations, such as the heating dependent red-shift and effects of geometrical variability, as discussed below. The computational model (see the ESI for more information†) based on Au[32] NPs arranged along a helical geometry was similar to the experimental system, given by a two turn helix of radius 50 nm and pitch 150 nm. We have considered spherical NPs of sizes that were similar to those of the (heated) experimental system, and have investigated the effects of variation of size and spacing of the NPs. Before discussing the simulation results, it is important to note an important difference between the experimental system and the

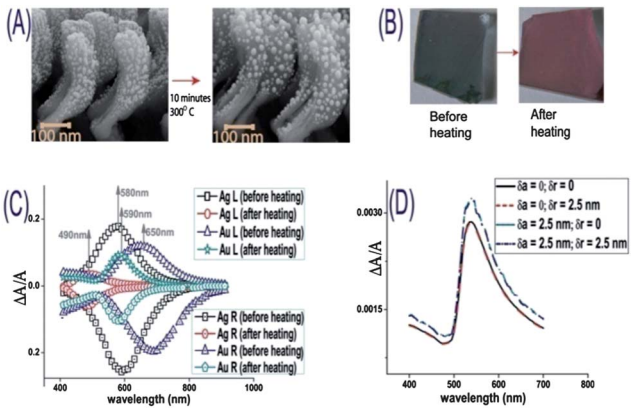

Fig. 2 (A) Change of shape (increased sphericity) of the NPs decorating the helices upon heating. (B) Change of color of the substrates (white light illumination) upon heating. (C) Blue-shift and reduction of the spectral width of the chiro-optical spectrum upon heating for Ag- and Au-decorated SiO_2 helical films. (D) Theoretical chiro-optical spectra for different variations of the size and spacing of the NPs. See text and ESI for details.†

geometries considered here. The average spacing to size ratio (r/a) between the NPs was chosen to be 4.6 in the simulation, thus assuming particles to be farther than those in the experimental system (r/a less than 3), which could have important consequences on the strength and shape of the chiro-optical signal. As the total number of NPs and their densities in the theoretical model were lower than the experimental system, it is reasonable that the anisotropy factors obtained were somewhat weaker than what was experimentally observed. The shapes of the chiro-optical spectra were similar to those observed in the experiments, and most interestingly, the effects of variance in NP size and spacing had a limited effect on the chiro-optical response (the average r/a was the same), as observed in the various spectra shown in Fig. 2D, provided r/a was greater than three. Assuming the same underlying dielectric template, for variation of $\delta a/a \sim 50\%$ and $\delta r/r \sim 50\%$, the chiro-optical spectra remained almost invariant, thus implying the suitability of this fabrication method to develop a well-designed optical material.

The fabrication method described here provides a novel platform to study plasmonic interactions in a wide variety of three-dimensional geometries. As an example, we have considered two 3D shapes each comprised of two helical constituents of slightly different pitch (700 nm and 400 nm), where the helical components were of the same handedness (R–R) in one, and opposite (R–L) in the other example. Schematic geometries and the SEM images of the two examples are shown in Fig. 3A. Evaporation of a thin layer of Ag or Au with a subsequent heating step resulted in the decoration of the R–R and R–L helices with spherical NPs with an average size of 20 nm and a mean spacing of 25 nm. Although the theoretical model assumed a spacing (21 nm) to size (14 nm) ratio larger than the experimental system, the overall shapes of the chiro-optical spectra are in agreement. The dramatic reduction of the chiral anisotropy factor in the R–L geometry is in agreement with the recent demonstration of additive properties of CD observed in plasmonic diastereomers. Due to negligible near field coupling between the chiral centers in the present geometry, the resultant chiro-optical property of the nanostructure was a sum of the contribution from individual helical constituents. This points towards the possibility of obtaining highly customized optical response by designing the individual building blocks judiciously.

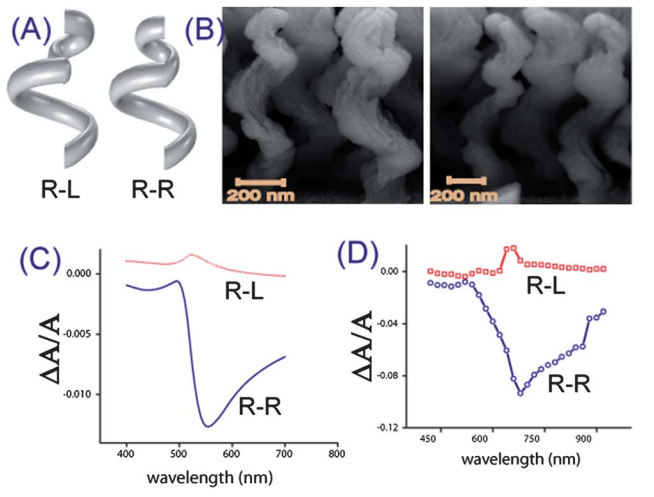

Fig. 3 (A) and (B) Schematic and SEM images of 3D structures (dielectric template only) made of R–R and R–L helical constituents. (C) and (D) Theoretical and experimental chiro-optical spectra of the R–R and R–L geometries, after decoration with NPs. See text and ESI for more details.†

Conclusions

In conclusion, the simple and versatile method described here could be used to fabricate strongly chiroptical metamaterials with high spectral tunability by simply changing the film thickness of the metallic layer, with or without a subsequent heating step. As the method is wafer scale with a very large number of helices interacting with an incident light beam, the differences between individual constituent components get averaged out; so different sections of the wafer demonstrate similar optical response. The yield of this technique is high where the wafer scale devices could be fabricated in a single fabrication run, requiring no pre- or post-processing steps. The inherent porosity and three-dimensional structures of the films make this material an attractive and new candidate to investigate the enhancement of chiroptical signals from optically active molecules in the strongly twisted[33,34] electromagnetic fields around metal coated helices. The most attractive feature of this technique is the possibility of experimentation with a wide range of helical, as well as various other geometries,[35] which provide an exciting new platform to study and engineer the dependence of plasmonic interactions on geometrical characteristics in great detail.

Acknowledgements

The authors thank N. Ravishankar and Subhaijit Kundu for their help with the microscopy images, Santhanam Venugopal for his help with the optical measurement system, Department of Biotechnology (DBT), Space Technology Cell (STC) and Aeronautical Development Agency (ADA-NPMASS) for funding this work, and gratefully acknowledge the usage of the facilities in Advanced Facility for Microscopy and Microanalysis (AFMM) and Micro and Nano Characterization Facility (MNCF, CeNSE) at IISc. This work is partially supported by the Ministry of Communication and Information Technology under a grant for the Centre of Excellence in Nanoelectronics, Phase II.

Notes and references

1 L. D. Barron, *Molecular light scattering and optical activity*, Cambridge University Press, 2004.
2 N. Liu, H. Guo, L. Fu, S. Kaiser, H. Schweizer and H. Giessen, *Nat. Mater.*, 2007, **7**, 31–37.
3 C. M. Soukoulis and M. Wegener, *Nat. Photonics*, 2011, **5**, 523–530.
4 J. B. Pendry, *Science*, 2004, **306**, 1353–1355.

5 S. Zhang, Y.-S. Park, J. Li, X. Lu, W. Zhang and X. Zhang, *Phys. Rev. Lett.*, 2009, **102**, 23901.
6 J. K. Gansel, M. Thiel, M. S. Rill, M. Decker, K. Bade, V. Saile, G. von Freymann, S. Linden and M. Wegener, *Science*, 2009, **325**, 1513–1515.
7 E. Hendry, T. Carpy, J. Johnston, M. Popland, R. V. Mikhaylovskiy, A. J. Lapthorn, S. M. Kelly, L. D. Barron, N. Gadegaard and M. Kadodwala, *Nat. Nanotechnol.*, 2010, **5**, 783–787.
8 A. Guerrero-Martínez, J. L. Alonso-Gómez, B. Auguié, M. M. Cid and L. M. Liz-Marzán, *Nano Today*, 2011, **6**, 381–400.
9 C. Helgert, E. Pshenay-Severin, M. Falkner, C. Menzel, C. Rockstuhl, E.-B. Kley, A. Tünnermann, F. Lederer and T. Pertsch, *Nano Lett.*, 2011, **11**, 4400–4404.
10 M. Hentschel, M. Schaferling, T. Weiss, N. Liu and H. Giessen, *Nano Lett.*, 2012, **12**, 2542–2547.
11 A. H. S. Oh, S. Liu, H. S. Jee, A. Baev, M. T. Swihart and P. N. Prasad, *J. Am. Chem. Soc.*, 2010, **132**, 17346–17348.
12 J. George and K. G. Thomas, *J. Am. Chem. Soc.*, 2010, **132**, 2502–2503.
13 A. Guerrero-Martínez, B. Auguié, J. L. Alonso-Gómez, Z. Džolić, S. Gómez-Graña, M. Žinić, M. M. Cid and L. M. Liz-Marzán, *Angew. Chem., Int. Ed.*, 2011, **50**, 5499–5503.
14 A. Kuzyk, R. Schreiber, Z. Fan, G. Pardatscher, E. M. Roller, A. Högele, F. C. Simmel, A. O. Govorov and T. Liedl, *Nature*, 2012, **483**, 311–314.
15 M. Decker, M. Ruther, C. E. Kriegler, J. Zhou, C. M. Soukoulis, S. Linden and M. Wegener, *Opt. Lett.*, 2009, **34**, 2501–2503.
16 M. M. Hawkeye and M. J. Brett, *J. Vac. Sci. Technol., A*, 2007, **25**, 1317–1335.
17 J. J. Steele and M. J. Brett, *J. Mater. Sci.: Mater. Electron.*, 2007, **18**, 367–379.
18 K. Robbie, M. J. Brett and A. Lakhtakia, *Nature*, 1996, 384.
19 Y. J. Liu, H. Y. Chu and Y. P. Zhao, *J. Phys. Chem. C*, 2010, **114**, 8176–8183.
20 J. G. Fan and Y. P. Zhao, *Langmuir*, 2008, **24**, 14172–14175.
21 H. J. Singh and A. Ghosh, *J. Phys. Chem. C*, 2012, **116**, 19467–19471.
22 C. Andy van Popta, C. S. Jeremy and M. J. Brett, *Appl. Opt.*, 2004, **43**, 3632–3639.
23 T. R. Jensen, M. D. Malinsky, C. L. Haynes and R. P. Van Duyne, *J. Phys. Chem. B*, 2000, **104**, 10549–10556.
24 B. J. Y. Tan, C. H. Sow, T. S. Koh, K. C. Chin, A. T. S. Wee and C. K. Ong, *J. Phys. Chem. B*, 2005, **109**, 11100–11109.
25 Z. Fan and A. O. Govorov, *Nano Lett.*, 2010, **10**, 2580–2587.
26 P. J. Flatau and B. T. Draine, *J. Opt. Soc. Am. A*, 1994, **11**, 1491–1499.
27 V. A. Markel, *J. Mod. Opt.*, 1993, **40**, 2281–2291.
28 Z. Fan and A. O. Govorov, *J. Phys. Chem. C*, 2011, **115**, 13254–13261.
29 N. A. Abdulrahman, Z. Fan, T. Tonooka, S. M. Kelly, N. Gadegaard, E. Hendry, A. O. Govorov and M. Kadodwala, *Nano Lett.*, 2012, **12**, 977–983.
30 A. O. Govorov and Z. Fan, *ChemPhysChem*, 2012, **13**, 2551–2560.
31 L. Zhao, K. L. Kelly and G. C. Schatz, *J. Phys. Chem. B*, 2003, **107**, 7343–7350.
32 P. B. Johnson and R. W. Christy, *Phys. Rev. B: Solid State*, 1972, **6**, 4370.
33 Y. Tang and A. E. Cohen, *Phys. Rev. Lett.*, 2010, **104**, 163901.
34 Y. Tang and A. E. Cohen, *Science*, 2011, **332**, 333–336.
35 N. Liu, H. Liu, S. Zhu and H. Giessen, *Nat. Photonics*, 2009, **3**, 157–162.